Diffuse Phase Transition and Phase Separation in Cr-Doped $Nd_{1/2}Ca_{1/2}MnO_3$: A Relaxor Ferromagnet

T. Kimura,[1] Y. Tomioka,[1] R. Kumai,[1] Y. Okimoto,[1] and Y. Tokura[1,2]
[1]*Joint Research Center for Atom Technology (JRCAT), Tsukuba 305-0046, Japan*
[2]*Department of Applied Physics, University of Tokyo, Tokyo 113-0033, Japan*
(Received 19 May 1999)

We have investigated the diffuse phase transition accompanying the formation of submicrometric ferromagnetic-metallic (FM) domains embedded in the antiferromagnetic charge-ordered state in $Nd_{1/2}Ca_{1/2}MnO_3$ crystals, which is caused by quenched random field originating from Cr impurities substituted on the Mn sites. The fraction of the FM phase volume or the size of the FM cluster can be controlled to a large extent by the magnetic-field annealing as well as the Cr content. The observed phenomena are reminiscent of those of relaxor ferroelectrics composed of ferroelectric clusters embedded in paraelectric matrix.

PACS numbers: 75.30.Vn, 75.30.Kz, 75.60.Nt

Transition-metal oxides with perovskite-related structure show a variety of gigantic-response phenomena such as ferroelectricity, colossal magnetoresistance, and high-temperature superconductivity. Recent extensive efforts to understand their mechanisms have revealed that the local inhomogeneity of the electronic/lattice structure often plays a crucial role in the properties. One of the well-known but still controversial issues is roles of the formation of charge and spin stripes and relevant electronic phase separation in doped nickelates, cuprates, and manganites. Among them, mixed-valent manganites, $R_{1-x}A_xMnO_3$ (R = La, Pr, Nd, and Sm; A = Sr and Ca), show charge-spin-orbital ordering near the doping level of $x = 1/2$ [1,2], and exhibit various magnetic-field induced phenomena due to the competition between the charge-orbital ordered (CO-OO) antiferromagnetic (AF) phase and the double-exchange ferromagnetic-metallic (FM) phase. Conspicuous phase transition from a CO-OO state to a FM one is caused by application of external stimuli such as magnetic field H [3], which has been attracting great interest in the context of unconventional phase control of the magnetic and electronic states in the magnetic oxides [4].

Recently, Raveau and his co-workers found that a small amount of transition-metal element substituted on Mn sites of the CO-OO manganites has a strong influence on the magnetic and electronic properties [5,6]. In particular, only a few percent of Cr substitutes suppress the CO-OO state and make the system ferromagnetic-metallic. The Cr impurities (Cr^{3+} with electronic configuration of $t_{2g}^3 e_g^0$ and spin quantum number $S = 3/2$) may produce not only localized holes but also immovable e_g-orbital deficiencies on the Mn sites.

In the light of electronic phase separation [7,8] and magnetic-field control of it, the effect of Cr substitution has been investigated here on the electronic and magnetic properties in a CO-OO AF insulating crystal of $Nd_{1/2}Ca_{1/2}MnO_3$. We detect the impurity-induced FM phase which appears in the CO-OO insulating matrix and grows in fraction by the magnetic-field annealing procedure. The observed magnetic and transport phenomena in the manganites are comparable with the dielectric phenomena in *relaxor ferroelectrics* which have been extensively studied for years because of importance in application as well as interest in the interplay between microstructure and dielectric properties [9]. We propose here that the impurity-induced insulator-to-metal transition in CO-OO manganites is likely described by a random field interaction scheme [10] which is a promising model for the mechanism of the diffuse phase transition in the relaxor ferroelectrics [11].

The electronic phase diagram of $Nd_{1/2}Ca_{1/2}MnO_3$ investigated here is similar to that of $Pr_{1/2}Ca_{1/2}MnO_3$ [3]. The ground state of $Nd_{1/2}Ca_{1/2}MnO_3$ is a CO-OO AF insulator in which the real space ordering of 1:1 Mn^{3+}/Mn^{4+} ions takes place at $T_{CO} \approx 250$ K. Upon the charge ordering, $d_{3x^2-r^2}/d_{3y^2-r^2}$ orbitals on the Mn^{3+} sites are alternately ordered in the ab plane. Below $\sim$170 K, local spin moments are antiferromagnetically ordered [12,13]. A large H more than $\sim$200 kOe is needed to melt the CO-OO AF insulating state in a neat (undoped) $Nd_{1/2}Ca_{1/2}MnO_3$ crystal [12].

$Nd_{1/2}Ca_{1/2}Mn_{1-y}Cr_yO_3$ ($0 \leq y \leq 0.1$) crystals investigated here were grown by the floating zone method. Inductively coupled plasma spectrometry on the grown crystals indicated that the stoichiometry is close to the prescribed ratio with accuracy of y within ± 0.002. The μm-scale homogeneity of Cr distribution was verified by an energy dispersive x-ray analysis. We performed both powder and single-crystal x-ray diffraction (XRD) measurements of the obtained crystals in a temperature range from room temperature to $\sim$20 K. Powder XRD data at room temperature show that all of the samples are of single phase and the *Pbnm* orthorhombic structure whose lattice parameters are nearly independent of the Cr content [14].

We display in the inset of Fig. 1 the temperature profiles of the resistivity measured by a four-probe

 0031-9007/99/83(19)/3940(4)$15.00

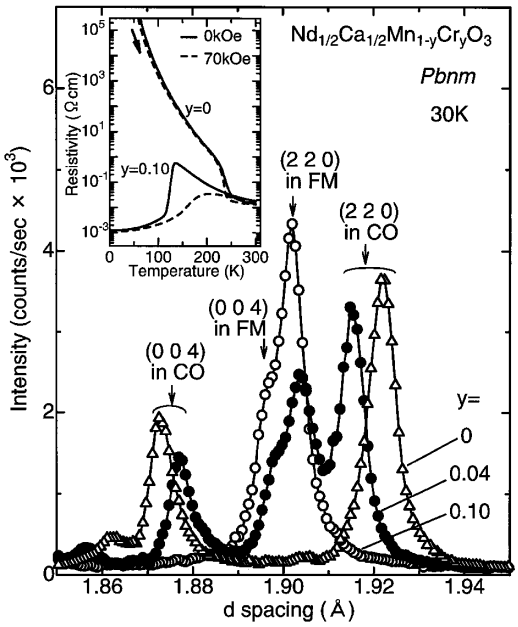

FIG. 1. X-ray powder diffraction patterns around the (004) and (220) Bragg peaks in $Nd_{1/2}Ca_{1/2}Mn_{1-y}Cr_yO_3$ ($y = 0$, 0.04, and 0.10) at 30 K. Inset: Temperature dependence of resistivity for crystals with $y = 0$ and 0.10 at 0 and 70 kOe.

method for $Nd_{1/2}Ca_{1/2}Mn_{1-y}Cr_yO_3$ crystals ($y = 0$ and 0.10) in $H = 0$ and 70 kOe. In the $y = 0$ crystal, a steep rise of resistivity can be observed around 230–250 K. The anomaly corresponds to the charge and orbital ordering transition. Single-crystal XRD measurements confirmed the presence of the superlattice reflections with modulation wave vector $(\sim 1/2, 0, 0)$ or $(0, \sim 1/2, 0)$, which can be attributed to the $d_{3x^2-r^2/3y^2-r^2}$ orbital ordering of Mn^{3+}. By contrast, the $y = 0.10$ crystal does not show such an anomaly around 240 K and instead the abrupt drop of the resistivity can be seen at $T_C \approx 130$ K. Compared with the magnetization data, the steep drop of resistivity is related to the onset of FM transition. The collapse of the CO-OO state by Cr doping is in good agreement with the previous result for polycrystalline samples [5], although the resistivity value of $\sim 10^{-3}$ Ω cm at the ground state is considerably lower than that in polycrystalline samples and attained only in the present single-crystalline sample free from grain boundaries.

The main panel of Fig. 1 displays the powder XRD data of samples with selected Cr contents at 30 K, enough below T_C and T_{CO}. In the $y = 0$ sample which shows a clear CO behavior, a large split between (004) and (220) Bragg peaks is attributed to the OO state. By contrast, no split can be found in the FM phase of the $y = 0.10$ crystal. It is to be noted that both peaks related to FM and CO-OO phases coexist at intermediate Cr-dopant concentrations ($0.02 \leq y < 0.06$), as exemplified by the $y = 0.04$ case in Fig. 1. According to the Rietveld analysis of the x-ray patterns [15], the fraction of the FM phase is systematically increased with the increase of Cr concentration, e.g., ≈19% for $y = 0.02$ and ≈38% for the $y = 0.04$ sample. These results demonstrate that each phase has a coherence length larger than the intrinsic coherence length for x-ray (a few hundred nm), and their relative portions vary with the Cr-doping level.

In the following, we focus on the $y = 0.02$ crystal in which mass fraction of the FM phase is close to a threshold concentration for percolation in simple cubic lattice ($p_c \approx 16\%$) [16] and for the continuum percolation transition in the three dimensional system ($p_c \approx 14.5\%$) [17]. We display in Fig. 2(a) the temperature profiles of the resistance for a $y = 0.02$ crystal in various H [18]. The resistance shows an insulating behavior down to the lowest temperature at zero field. The charge ordering for the $y = 0.02$ crystal is barely discernible as a steep change in the resistance around $T_{CO} \approx 230$ K, while the OO-related superlattice structure is clearly observed below T_{CO} by single-crystal XRD measurements. The application of H drastically reduces the resistance below T_{CO} and makes the system semimetallic. The value of resistance at the ground state varies with the magnitude of H.

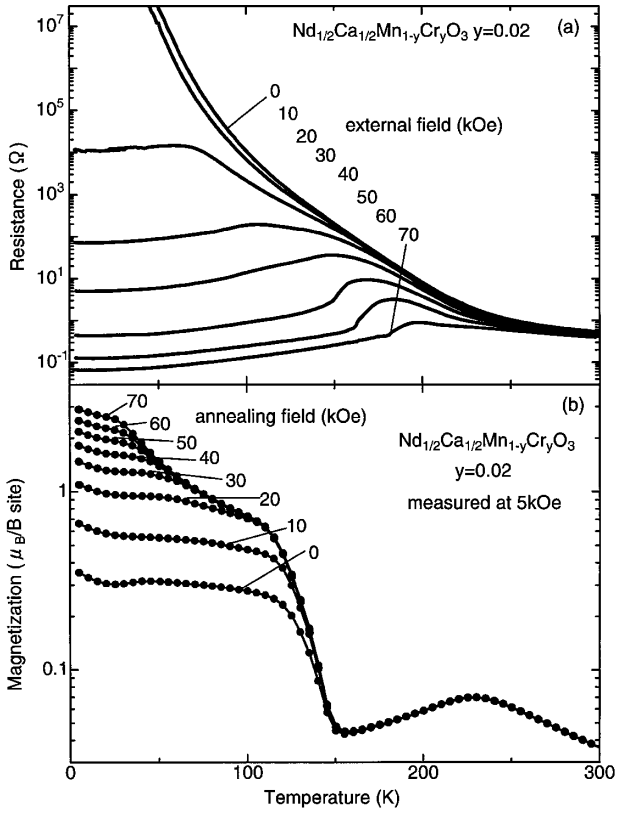

FIG. 2. (a) Temperature dependence of the resistance in various H for a crystal of $Nd_{1/2}Ca_{1/2}Mn_{1-y}Cr_yO_3$ ($y = 0.02$). The measurements were performed in a field-cooling run once the magnetic fields were applied at 300 K. (b) Temperature dependence of the magnetization in the warming run at 5 kOe for the $y = 0.02$ crystal. The measurements were performed once the magnetic fields were applied at 300 K and the crystals were cooled in the respective annealing fields down to 5 K.

Figure 2(b) shows the magnetic-field annealing effect on the magnetization. For these measurements, the crystal was cooled from 300 to 5 K in the respective magnetic fields. Then the magnetization was measured by warming the crystal in a relatively small H (5 kOe). The anomaly at $\approx$230 K is observed in all the data and is related to the onset of the CO-OO transition in some portion of the crystal. In the temperature range above $\approx$150 K, no difference in the magnetization was observed. The steep rise of magnetization toward low temperature is observed at $\approx$150 K, which is attributed to the onset of ferromagnetic spin ordering. A striking feature in Fig. 2 is that the magnitude of the magnetization below T_C, or equivalently the fraction of the FM phase, is totally governed by the magnitude of annealing magnetic field.

To further examine such an anomalous magnetic-field annealing effect on the magnetic and transport properties, the annealing-field ($H_{\rm ann}$) dependencies of magnetization and resistance were measured at 5 and 4.2 K, respectively, as displayed in Figs. 3(a) and 3(b). For these measurements, the crystal was slowly cooled from 300 to 5 K (or 4.2 K) at various magnetic fields ($H_{\rm ann}$) in the respective runs, and then H was swept cyclically between $H = +H_{\rm ann}$ and $H = -H_{\rm ann}$. The traces with the change of field are represented by solid lines shown in Figs. 3(a) and 3(b). All magnetization curves are saturated at $H \approx 10$ kOe due to the domain rotation of the ferromagnetic cluster and show no discernible hysteresis. At the annealing magnetic field ($H_{\rm ann}$) of 10 kOe, the value of spontaneous magnetization ($\approx 0.6\mu_B$) is $\approx$15% of that of the almost fully FM $y = 0.10$ crystal, which is in good agreement with the FM fraction ($\approx$19%) estimated by the x-ray diffraction. The saturation moment steadily increases with the increase of $H_{\rm ann}$. The saturation magnetization at $H_{\rm ann} = 70$ kOe becomes comparable with that expected for the full Mn moment. In addition, the magnitude of resistance also drastically decreases with increasing $H_{\rm ann}$ [Fig. 3(b)]. With increasing $H_{\rm ann}$ from 0 to 70 kOe, the resistance changes by more than 6 orders of magnitude. However, once after temperature is lowered down to 4.2 K in a fixed $H_{\rm ann}$, the isothermal magnetoresistance effect [e.g., $\Delta\rho/\rho(70\ \text{kOe}) \sim 30\%$], which is perhaps related to the spin-dependent scattering at the interface between the CO-OO and FM domains, is rather minimal as compared with several orders of magnitude changes in resistance by the magnetic annealing effect. The systematic evolution of the saturation moment and the metallic conduction by the magnetic-field annealing can be attributed to the increase of fraction of the FM phase at the expense of the CO-OO phase volume. The fraction of FM phase is altered from $\sim$15% up to $\sim$100% by the increase of $H_{\rm ann}$ from 0 to 70 kOe in such a mixed-phase system, which results in the percolative conduction on the FM domains as observed.

We have also observed the long-time relaxation or aging effect of magnetization and conductance in such a phase-separated state. We display in Figs. 4(a) and 4(b) time dependencies of both quantities at selected temperatures, respectively. After zero-field cooling, the H of 40 kOe was at first applied to induce the local ferromagnetic order, and the magnetization and the conductance were recorded as a function of time. The magnetization increases slowly with increasing time, showing nearly logarithmic time dependence [solid lines in Fig. 4(a)]. In accordance with the increase of the magnetization, the increase of conductance was also observed with the increase of time. Such an aging effect arises from the slow evolution or growth of the FM cluster for the crystal kept at a constant temperature in a magnetic field.

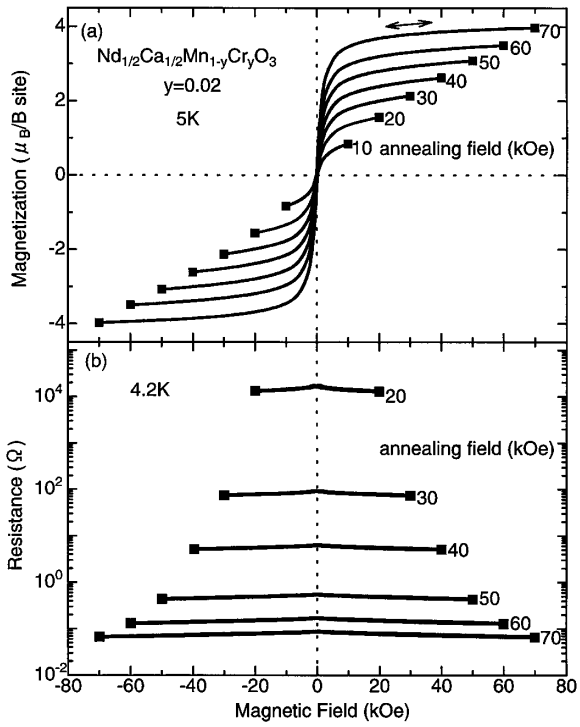

FIG. 3. Field dependence of (a) magnetization at 5 K and (b) resistance at 4.2 K for a $Nd_{1/2}Ca_{1/2}Mn_{1-y}Cr_yO_3$ ($y = 0.02$) crystal. The measurements were performed once the magnetic fields were applied at 300 K and the crystal was cooled to 5 K (or 4.2 K) in the respective annealing fields.

The presently observed phenomena such as magnetic-field annealing and aging effects on the temporal evolution of FM microembryos in the CO-OO AF matrix may remind us of the case of *relaxor ferroelectrics* [9] in which ferroelectric domains on a nanometric scale are embedded in a paraelectric matrix. Relaxor ferroelectrics are distinguished from ordinary ferroelectrics by a diffuse phase transition and strong frequency dependence of the dielectric properties. They also show electric-field annealing and aging effect on the optical birefringence effect [11,19], which corresponds to the evolution of micropolar clusters by an external electric field. Although most of the relaxor ferroelectrics in perovskites are lead (Pb) based compounds with alloyed heterovalent B sites

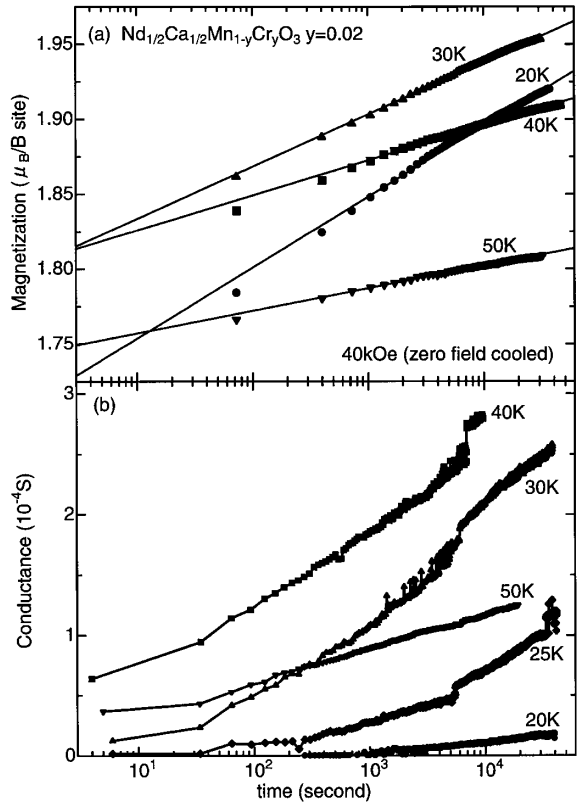

FIG. 4. Temporal profiles of (a) magnetization and (b) conductance in $H = 40$ kOe at various temperatures for a $Nd_{1/2}Ca_{1/2}Mn_{1-y}Cr_yO_3$ ($y = 0.02$) crystal. The crystal was at first cooled at zero field from room temperature to the respective temperatures and then the H was applied.

expressed as $Pb(B, B')O_3$, diluted impurity systems like $K_{1-x}Li_xTaO_3$ and $Sr_{1-x}Ca_xTiO_3$ also exhibit all of the above typical properties. One of the promising models for explaining the diffuse transition of relaxor ferroelectrics is the random-field interaction scheme [10], which is based on the assumption that the quenched random electric fields are caused by random distribution of different ions on A or B sites [11].

The above model considering the quenched random field seems to approximately apply as well to the present manganese oxide in which Cr impurities induce the local CO/OO-to-FM transition. Since the Cr^{3+} ($t_{2g}^3 e_g^0$) is chemically stable, the e_g-like conduction electron may not move onto the Cr site and the Cr site serves as the immobile e_g orbital deficiency. Such a fixed orbital deficiency may be viewed as the quenched random field in the charge and orbital sectors, and hence may destroy the orbital ordering and produce the FM microembryos. The FM microclusters with Cr nuclei may grow, be connected with each other, and be transformed into the FM domains on a large scale ($>10^3$ Å), e.g., by increasing the Cr-doping level to $y \approx 0.04$ or by applying the annealing field for $y \approx 0.02$.

In summary, the impurity-induced insulator-to-metal transition has been investigated for the charge-orbital ordered antiferromagnetic crystals of $Nd_{1/2}Ca_{1/2}MnO_3$. We propose that the impurity-substituted manganite can be viewed as the *relaxor ferromagnet.* The impurity produces the ferromagnetic-metallic microembryos whose mass fraction increases in the charge-orbital ordered insulating matrix with the increase of doping level as well as by the field-annealing procedure. The conspicuous magnetic-field annealing and aging effects on the growth of the ferromagnetic domain are observed for the Cr-doped (e.g., 2%) $Na_{1/2}Ca_{1/2}MnO_3$ composed of charge-orbital ordered phase and ferromagnetic-metallic one, which enables us to control the magnitude of magnetization and conductance to a considerable extent (up to an almost fully ferromagnetic and metallic state). The quenched random field in the spin, charge, and orbital sectors originating from a few percentage of Cr impurity is likely responsible for all the characteristics of a relaxor ferromagnet, such as the diffuse phase transition, the history-dependent appearance and growth of ferromagnetic-metallic clusters, and the resulting insulator-to-metal transition.

We thank N. Nagaosa and A. Yamanaka for helpful discussions. This work was supported in part by NEDO.

[1] E. O. Wallan and W. C. Koehler, Phys. Rev. **100**, 5455 (1955).
[2] Z. Jirak *et al.*, J. Magn. Magn. Mater. **53**, 153 (1985).
[3] Y. Tomioka *et al.*, Phys. Rev. B **53**, R1689 (1996).
[4] For a review, see, for example, *Colossal-Magnetoresistive Oxides*, edited by Y. Tokura (Gordon & Breach Science Publishers, New York, 1999).
[5] A. Barnabe *et al.*, Appl. Phys. Lett. **71**, 3907 (1997).
[6] B. Raveau *et al.*, J. Solid State Chem. **130**, 162 (1997).
[7] A. Moreo *et al.*, Science **283**, 2034 (1999).
[8] M. Uehara *et al.*, Nature (London) **394**, 560 (1999).
[9] For review see L. E. Cross, Ferroelectrics **76**, 241 (1987); **151**, 305 (1994).
[10] Y. Imry and S.-K. Ma, Phys. Rev. Lett. **35**, 1399 (1975).
[11] V. Westphal *et al.*, Phys. Rev. Lett. **68**, 847 (1992).
[12] M. Tokunaga *et al.*, Phys. Rev. B **57**, 5259 (1998).
[13] T. Vogt *et al.*, Phys. Rev. B **54**, 15 303 (1996).
[14] The unit-cell parameters of the $y = 0$ sample were $a = 5.3828(1)$ Å, $b = 5.4064(2)$ Å, $c = 7.5980(2)$ Å, while those of the $y = 0.10$ sample were $a = 5.3796(2)$ Å, $b = 5.4011(2)$ Å, $c = 7.5983(3)$ Å at room temperature.
[15] F. Izumi, *Rietveld Method*, edited by R. A. Young (Oxford University Press, Oxford, 1993), Chap. 13.
[16] H. Scher and R. Zallen, J. Chem. Phys. **53**, 3759 (1970).
[17] I. Webman *et al.*, Phys. Rev. B **14**, 4737 (1976).
[18] The magnitude of low-temperature resistivity at zero field critically depends on the samples taken from the same batch with the composition of $y \approx 0.02$. Some crystals show a barely metallic behavior below $\sim$100 K. The results suggest that the insulator-metal transition in the system is near the percolation threshold.
[19] K. Fujishiro *et al.*, J. Korean Phys. Soc. **32**, S964 (1998).